Received: 22 December 2017 | Revised: 27 March 2018 | Accepted: 20 April 2018

DOI: 10.1002/fam.2635

SPECIAL ISSUE PAPER

WILEY

Study of fire behaviour of facade mock-ups equipped with aluminium composite material-based claddings, using intermediate-scale test method

Eric Guillaume[1] | Talal Fateh[2,3] | Renaud Schillinger[1] | Roman Chiva[1] | Sebastian Ukleja[2]

[1] Efectis France, route de l'Orme des Merisiers, 91193 Saint Aubin Cedex, France

[2] Efectis UK-Ireland, Jordanstown Campus Block 27, Shore Road, Newtownabbey BT 37 0QB, UK

[3] Ulster University, FIRESERT, Jordanstown Campus Block 27, Shore Road, Newtownabbey BT 37 0QB, UK

Correspondence
Eric Guillaume, Efectis France, route de l'Orme des Merisiers, 91193 Saint Aubin Cedex, France.
Email: eric.guillaume@efectis.com

Summary

The fire behaviour of a building façade is dependent on the overall system's performance, rather than the performance of the individual components. A façade system includes the cladding and the insulant's characteristics, but also the cavities, cavity barriers, mounting and fixings, substrate, and any singularities, such as window frames. This publication presents façade fire propagation test according to the ISO 13785-1 standard, with additional heat release rate and gases analysis using FTIR. Tests have been performed on 9 different compositions of aluminium composite panels (ACM) with several insulants. For tested compositions, the cladding is the most important parameter driving global fire behaviour of façade mock-ups. ACM-PE-based cladding systems gave very different results from the other solutions tested. This was especially visible in heat release rates, where fire intensity was very high, whatever the insulant used in the system. The contribution of the insulant was only remarkable in these tests during the decay phase. The cavity barrier was largely ineffectual in the 3 tests with ACM-PE cladding, as the integrity of the cavity was not ensured.

KEYWORDS

façade fires, intermediate-scale testing, fire behaviour, gases evolved, heat released

1 | INTRODUCTION

Aluminium composite materials (ACMs) are increasingly commonly used as cladding when designing building facades nowadays, but different types of cladding can achieve very different levels of performance.

Assessment of a particular façade system's fire performance can be undertaken using large-scale testing in accordance with BS8414-1, but there is currently no commonly accepted method of extending the scope of a large-scale tested system, to account for variances from the configuration that has been tested; it is therefore proposed that intermediate testing could allow a route for assessing the significance of different system configurations and components to extend the scope of large-scale tested systems.

The test protocol proposed for such intermediate level testing is a façade fire propagation test according to the ISO 13785-1 standard, with additional heat release rate and gases analysis using FTIR. Tests results have been compared with real-scale data available to estimate measurement relevance of such intermediate-scale tests.

In order to appreciate the variability of different system configurations, as well as the effect of different interactions between panels and insulants, a test campaign of 9 combinations of cladding and insulants was performed using intermediate level testing; this involved 3 different ACM-based cladding systems in combination with 3 different insulants within each system.

The global market for façade insulation and especially ventilated facades is growing quickly and likely to double in size by 2024.[1] In this growing market, the proportion of ACMs is currently estimated as

25% of the market share for US and the same level for Europe.[2] Such global and increasing use of ACMs requires proper risk evaluation.

Façade systems have been implemented on a great many commercial and residential buildings, providing a good level of energy efficiency, weather resistance, and improved aesthetics. ACM cladding is generally followed by a cavity, then the insulant, over the face of a building structure (often either a steel frame or masonry or concrete framed substrate). The construction products used as external façade assemblies may include combustible insulants and combustible claddings. As stated in Table 1, there have been several significant fires over the last decade involving rainscreen facades; a large proportion of these have been involved in the use of a combustible ACM-based cladding. Such fires are described in Valiulis,[3] White and Delichatsios,[4] and White et al[5] and have been involved in massive fatalities and property losses. According to the table, propagation through the cladding and penetration from the outside to the inside are the most important parameters driving these fires and their consequences.

2 | CONTEXT AND EXISTING FAÇADE TEST RESULTS

After the Grenfell tragedy in June 2017,[6] the UK government commissioned 7 large-scale BS8414-1[7] tests in order to determine which types of insulation could safely be used with different cladding types. These tests were performed by the BRE, according to criteria from BR135 document.[8] The test campaign involved 3 types of cladding: ACM with a polyethylene dominated core from here on referred to "ACM-PE" (this is the type that was used on Grenfell tower), Fire retardant ACM cladding, with a better fire performance, hereafter referred to as "ACM FR," and ACM cladding with a mineral core filling of limited combustibility, hereafter referred to as "ACM A2". These cladding types were initially tested in combination with a PIR insulant as used at Grenfell and a Mineral wool insulant. Test results[9,10-13,14,15] are summarised in Table 2. None of the ACM-PE-based compositions passed the test. Unfortunately, BS8414 tests give very little quantitative information for further interpretation of fire behaviour of these systems. Moreover, the tests were extinguished as soon as BR135 criterion failed, making a complete fire scenario (growth, possible plateau, and decay of the fire) impossible to assess.

An additional test was undertaken with ACM-FR and phenolic insulation.[16] The rationale for this was that not all plastic foams are alike. It was conceivable that a phenolic insulant could pass the test with FR-grade cladding, even if PIR did not. The phenolic did perform a little better than the PIR—but it still failed. The phenolic was deemed to have failed the test after 28 minutes. The equivalent PIR test lasted just 25 minutes, both met all temperature criteria set out in BR135; however, they both failed due to "flames on top of the rig". Looking at the reports test pictures, it is clear that, although it passed, the mineral wool insulation with the ACM FR barely only passed the criteria "flames on top of the rig".

FM Global recently undertook a series of tests on ACM-based panels, according to a 16 feet parallel panel test stated in ANSI/FM4880.[17] Results were then compared with NFPA 285.[18] A large number of façade systems were evaluated. The results were sufficient for FM Global to take a view that the ANSI/FM 4880 parallel panel test method was discriminant enough to identify hazardous assemblies. Compared with NFPA 285, several compositions that complied

TABLE 1 Recent façade fire events involving ACM claddings

Date	Place	Circumstances and Consequences
1/10/2010	Wooshin Golden Suites, Busan, South Korea	No fatalities, 5 injured. Fire from apartment, propagated by the façade.
14/5/2012	Roubaix, France	Dwelling building fire, 1 fatality, 20 apartments (over 94) destroyed. Initiated from apartment fire, propagated through decorative ACM panels on balconies
17/7/2012	Polat Tower, Istanbul, Turkey	Fire caused by a faulty air conditioning unit, no fatalities.
18/11/2012	Tamweel (Al Seef) Tower, Dubai, UAE	No fatalities. The building was made uninhabitable by the fire and is expected to be reconstructed
3/4/2013	Hotel and Business Center, Grozny, Chechnya	Fire completely destroyed the plastic trimming used on the building's exterior, but the interior remained untouched.
25/11/2014	Lacrosse Tower, Melbourne, Australia	No fatalities or serious injuries. Levels 6 to 21 were affected by fire, and many more were affected by water damage.
21/2/2015	Marina Torch Tower, Dubai, UAE	7 injuries. The fire started in the middle of the building and spread rapidly due to falling flaming debris and high winds. External cladding was charred from the 50th floor (over 82) to the top of the tower
19/5/2015	Dwelling building, Baku, Azerbaijan	16 fatalities, 63 injuries. Fire propagated on façade after a renovation.
1/10/2015	Nasser Tower, Sharjah, UAE	19 injuries. Fire started on the third storey and moved up through the façade.
31/12/2015	Hotel The Address, Dubai, UAE	No fatalities. Fire started outside the 20th floor of the hotel but did not spread inside.
14/06/2017	Grenfell tower, London	71 fatalities. Initiated from an apartment fire, rapid propagation to the façade and penetration from the outside to the other storeys
4/8/2017	Marina Torch Tower, Dubai, UAE	Second fire on the same tower. No fatalities. Debris from the fire falling to the ground and starting a second fire in the streets below.
22/12/2017	Dwelling building, Jecheon, South Korea	29 fatalities. Initiated from a car fire in underground car park, then propagated to the cladding

TABLE 2 Results of BRE tests after Grenfell disaster

BS8414-1 Tests	With Combustible Insulant (PIR)	With Mineral Wool Insulant
Aluminium with mineral core ACM A2	Pass	Pass
Aluminium with fire-retardant core ACM FR	Fail at 25 min	Pass
Aluminium with polyethylene core ACM-PE	Fail at 8 min	Fail at 7 min

with this standard did not pass the parallel panel test, mainly because of lower heat exposure in the NFPA 285 test compared with realistic façade fire scenarios.

Large-scale and real-scale façade experiments such BS8414-1 are however expensive and take a long time to prepare. As a consequence, there is a need for an intermediate test method able to be correlated with a large-scale reference test to account for variations from what is tested at a larger scale. An example of application is to extend reference tests with small changes in geometry or thicknesses of a component, and to validate this extended application using a scientifically based assessment. The test campaign described hereafter in this publication intends to cover this need, consider sensitivity, and identify whether an intermediate-scale test method can be discriminant enough.

3 | DESCRIPTION OF TEST SETUP

A series of 9 tests were undertaken based on the ISO 13785-1 standard.[19] This test involves assessment of a medium-scale mock-up of facades. In this test façade, samples are fixed over a calcium-silicate board maintained on a steel frame. All the equipment is placed with wind screens on 3 faces made of Fire-rated plasterboards. A global arrangement is visible in Figure 1. The test arrangement is similar to a one third scale of BS 8414-1 test, with a 100-kW gas burner placed at the bottom of the back wing of the sample. The burner is a sand-diffusion propane burner of 100 kW, with a length of 1200 mm and a width of 100 mm and a height of 150 mm. Its upper surface is placed 250 mm below the lower edge of the sample. The complete system is then placed under a large hood to collect effluents.

For this testing, several deviations from ISO 13785-1 standardised test protocol were made:

- Test duration was systematically 30 minutes with burner on;
- Tests were performed under a large calorimetric hood. The heat release rate and smoke effluents rate were measured continuously according to ISO 24473[20];
- Smoke was collected for FTIR analysis of the effluents, according to ISO 16405[21] and ISO 19702.[22]

Depending on the energy release, 2 different sizes of calorimetric hood were used. The medium one was a 3 m × 3 m hood used as per ISO 9705 standard.[23] This allows good measurement conditions for heat release rates from 100 kW to approximately 3.5 MW. The larger one was a 9 m × 9 m hood, which allows good measurement conditions for heat release rates from 500 kW to 20 MW.

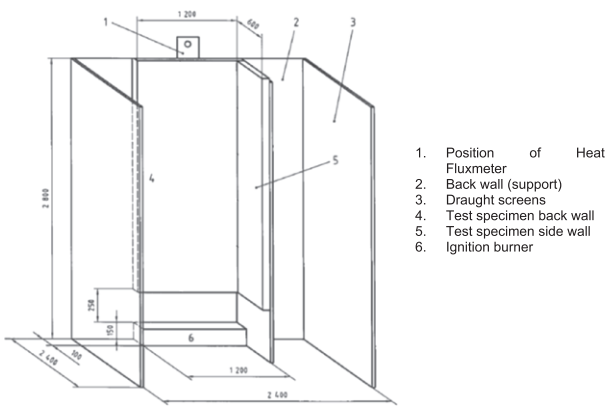

FIGURE 1 Description of test method general arrangement, as from standard. A, Sample design. B, Location of sensors

4 | DESCRIPTION OF SAMPLES

4.1 | Cladding

Three different ACM panels used as cladding were tested. References of the products are as follows:

- Alpolic A2 limited-combustibility cladding; Hereafter designed as "ACM-A2"
- Alpolic/fr-RF Reduced-combustibility cladding; Hereafter designed as "ACM-FR"
- Reynobond PE standard cladding with polyethylene core; Hereafter designed as "ACM-PE"

4.2 | Insulants

Three different insulants were used in combination with each of the cladding types for the test combinations, as follows:

- Kingspan K15 phenolic foam, hereafter designed as "K15". Thickness of the insulant was 50 mm
- Celotex RS5000 PIR hereafter designed as "PIR". Thickness of the insulant was 50 mm
- Mineral wool Rockwool Duoslab hereafter designed as "MW". Thickness of the insulant was 100 mm

Information regarding these insulants, such as density or thermal conductivity, is available on product datasheets from their respective manufacturers. The different thicknesses of combustible insulants or mineral wool were chosen to achieve similar levels of thermal performance. As the total thickness is different between organic foams and mineral wool compositions, burner position was adjusted in order to produce similar thermal attack to the cavity.

4.3 | Mounting and fixing

The insulant and the cladding were assembled on calcium silicate boards (860 kg/m^3) compliant to EN 13238[24] requirements, as seen in Figure 2 and as follows:

- Cladding made of panels of 779 × 508 mm (3 × 2 panels for back wall and 3 panels for side wall of test wing). Gaps between cladding panels are 20 mm wide;
- Cavity of 50 mm with intumescent cavity fire barrier above second rank of panels. At the position of the cavity barrier, the thickness of the cavity is reduced to 24 mm in this zone;
- Vertical frame made of aluminium profiles;
- Lower edge of the test frame is covered by a 2-mm-thick aluminium L profile, with a 20-mm airgap at the bottom panel and the angle.

4.4 | Test sequence

The 9 different combinations were tested at Efectis UK-Ireland, Belfast, in indoor facilities (no wind, constant temperature). The test description can be found in Table 3. The tests using ACM-FR and ACM-A2 compositions were performed under Efectis UK-Ireland intermediate scale hood (3 m × 3 m), similar to the hood described in ISO 9705-1 standard.[23] The tests using ACM-PE claddings were performed under Efectis UK-Ireland large hood (9 m × 9 m), with a limit of 20 MW. All tests were only performed once.

TABLE 3 Tested compositions

Tested Composition	Cladding	Insulant
Composition 1	ACM-FR	PIR
Composition 2		K15
Composition 3		MW
Composition 4	ACM-A2	PIR
Composition 5		K15
Composition 6		MW
Composition 7	ACM-PE	PIR
Composition 8		K15
Composition 9		MW

5 | DESCRIPTION OF MEASUREMENTS

5.1 | Temperatures and heat fluxes

Temperatures and heat fluxes measured were as described in ISO 13785-1.5 thermocouples were placed at the middle axis of the back wall of the sample. They are noted as L1 to L5, at respective heights from the base of the sample of 500, 1000, 1500, 2000, and 2400 mm (top of the sample). Similar thermocouples, noted S1 to S5, were placed on the middle axis of the side wall. All these surface

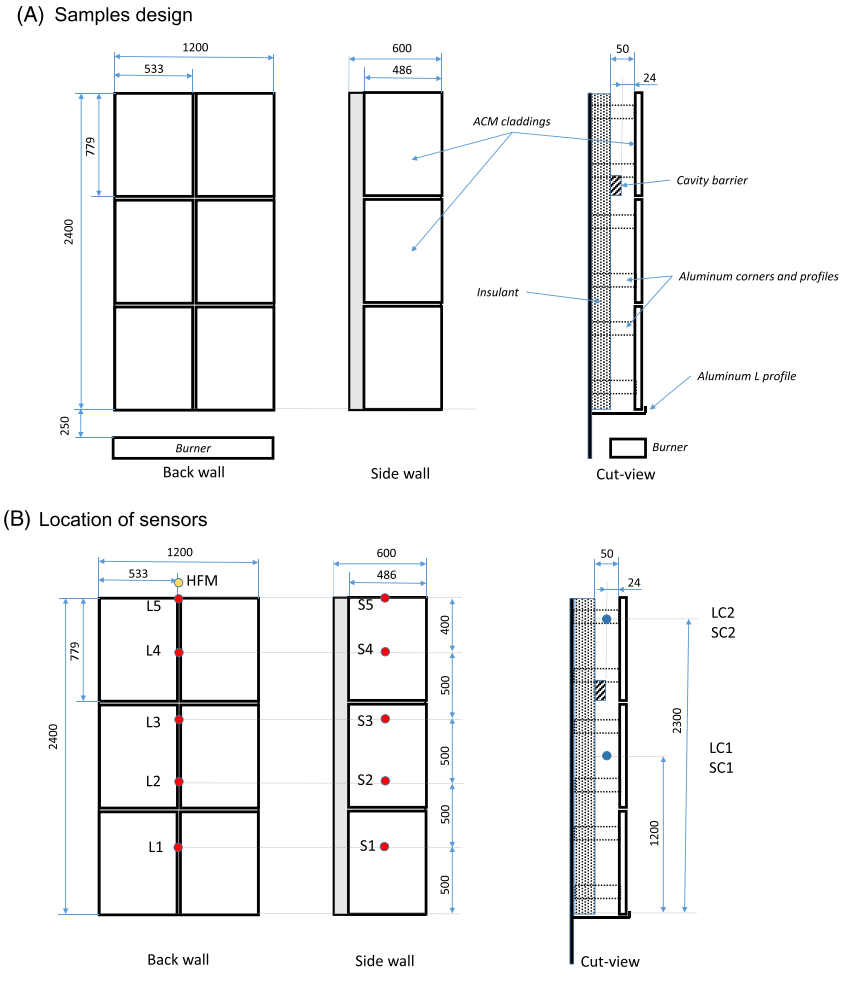

FIGURE 2 Description of test mock-ups and sensor positions [Colour figure can be viewed at wileyonlinelibrary.com]

temperatures were measured using surface thermocouples on 12-mm copper disks, K-type.

Additional thermocouples were placed in the middle of the cavityand each side of the cavity barrier, at respective heights of 1200 and 2300 mm from the base of the sample. They are noted, respectively, as LC1 and LC2 for the back wall, and SC1 and SC2 for the side wall. These thermocouples were Inconel shielded 1.5-mm K-type thermocouples.

Heat flux is measured using an Schmidt-Boelter gage sensor, sensitive to a combination of radiation and convection as described in ISO 14934-1:2010.25

Uncertainty in temperature measurement is evaluated as ±2.5 K. Uncertainty in heat flux measurement is evaluated as ±7%. Location of all these sensors is detailed in Figure 2.

5.2 | Heat release rate

Heat release rate, expressed in kW, is calculated using oxygen consumption method as proposed by Thornton[26] and modified by Huggett.[27] Carbon dioxide and carbon monoxide (CO) are also considered in the method to quantify the incomplete character of the combustion.[28]

In practice, resolution on heat release rate is driven by dilution and the size of the equipment. So, to allow accurate measurement, the size of the hood used and the flowrate in the duct have to be adapted to the expected heat release rate to obtain a depletion factor not exceeding 17% of oxygen in the effluents but being significantly different from initial. As a consequence, in this test campaign, 2 different hoods were used.

Both calorimeters used were checked using a reference gas burner able to represent the range of measurement expected.

Uncertainty of measurement of heat release rate is evaluated as ±10%.

5.3 | Smoke production rate

Smoke production rate is calculated according to light transmission method, using a He-Ne red laser opacimeter. Beam attenuation is expressed as extinction coefficient in m^{-1}. Smoke production rate is given by multiplying extinction coefficient by flow rate. It is expressed in m^2/s.

Uncertainty of measurement of smoke production rate is evaluated as ±20%.

5.4 | Gases evolved

5.4.1 | Quantitative analysis

Carbon monoxide (CO) and carbon dioxide (CO_2) are quantified in the main duct of each calorimeter using, respectively, a small electrochemical cell and a non-dispersive infrared analyser (NDIR). Signal expressed in µL/L (ppm) is then converted into mass release rate (in g/s) using smoke flow rate calculated as above. Analytical technique and expression of results are detailed in ISO 19701.[29]

Uncertainty of measurement of CO_2 concentration is evaluated as ±5%. Uncertainty of measurement of CO concentration is evaluated as ±10%. Limit of quantification is very dependent on flow rate and gas diffusion, and so on the calorimeter used.

5.4.2 | Qualitative analysis

Qualitative analysis and semi-quantitative assessment were undertaken using online FTIR. The FTIR measurements were performed with a Bruker Tensor 27 spectrometer set at a resolution of 1 cm^{-1} in the range 740 to 4000 cm^{-1}. The spectrometer was equipped with a MCT detector and a long path heated gas cell. The gas cell having the volume of 2.9 L was equipped with BaF_2 windows. The path was set at 1 m. The gas cell was heated at 180°C. Extraction rate was set at 3 L per minute. The gas cell was not equipped with an absolute pressure gauge, and only relative pressure was monitored—and kept as close as possible to ambient pressure. Equipment complied with ISO 19702[30] requirements.

The fire effluent was extracted by a stainless steel probe with a set of different diameter openings along the long axis to allow uniform extraction. The stainless-steel probe was fixed at right angle to the tested façade wall and connected to a 2.5-m-long heated pipe incorporating a heated filter (both kept at 200°C).

Full quantitative assessment is not possible with this equipment and sampling setup, but trends in concentrations represent the proper kinetics of analysis. The equipment was calibrated for the following components: carbon dioxide, CO, water vapour, hydrogen chloride, hydrogen bromide, hydrogen fluoride, hydrogen cyanide, sulphur dioxide, nitrogen dioxide, nitrogen monoxide, nitrogen protoxide, formaldehyde, ammonia, methane, ethane, ethylene, and acetylene. Water analysis is needed to correct from interferences. Ammonia, methane, ethylene, and acetylene are calibrated as they are frequent interfering species. These species are also released in pyrolysis phases. For example, acetylene and ammonia interfere with proper quantification of hydrogen cyanide. Additional components have been tested for qualitative assessment. This includes benzene, toluene, o-m-p xylene, styrene, acrylonitrile, acrolein, quinoline, propionaldehyde, toluidine, nitrobenzene, hexane, carbonyl sulphide, aniline, butadiene, acetonitrile, acetone, acrylic acid, vinylacetate, vinylchloride, phenol, methylmethacrylate, methanol, and acetaldehyde.

Due to the massive quantity of data produced by such equipment, only semi-quantitative assessment of identified species is detailed in this publication, without spectral data. The semi quantitative analysis was performed for the following gases found, using data from Guillaume and Saragoza31:

1) Carbon monoxide using Beer's law and absolute peak height in the range 2177.9 to 2174.5 cm^{-1}
2) Methane using Beer's law and relative peak height in the range 2951.1 to 2946.7 cm^{-1}
3) Ethylene using Beer's law and relative peak height in the range 2988.5 to 2987.6 cm^{-1} with baseline for this peak set between 2990.4 and 2984.5 cm^{-1}
4) Ethylene was further checked for possible cross-correlations with methane and/or ethane in that spectral region by performing additional semi-quantification using Beer's law and relative peak height in the range 954.6 to 943.1 cm^{-1}

6 | TEST RESULTS

6.1 | Observations

Figure 3A presents observations during tests. Roughly, the tests involving ACM-FR and ACM-A2 present close patterns vs time, with limited degradation sometimes visible inside the cavity but limited by the fire barrier.

Figure 3B presents observations of the insulant after the 3 tests involving ACM-PE claddings. The charring depth is similar for the 3 insulants, with traces of combustion at approximately 10 mm depth. This means that combustion occurred so quickly at the surface of the material, that the insulants contributed little to the combustion, and this contribution probably stopped after destruction of the cladding.

6.2 | Heat release

Table 4 details results of maximum heat release, as well as total heat release. The contribution of the burner was calculated on the basis of a propane flame of 100 kW during 30 minutes. Figures 4 to 7 present the different results for the 9 tests.

Maximum heat release rate from the tests with ACM-PE grew to almost 5 MW. This was similar for each of the ACM-PE tests and was more than 16 times higher than for all the other tests. This peak appears early, after only 4 minutes. The peak was of a short duration, only a few minutes. For the test involving the ACM-PE + MW, the heat release rate curve has a similar trend observed for the tests involving ACM-PE + K15 and ACM-PE + PIR, but the decay started earlier, meaning a probable small contribution from combustible insulants in the decay phase. This probably explains the difference seen between these 3 tests for total heat released. The peak of heat released is very intense but so short that in a test averaged during 30 minutes, the difference between the tests using ACM-FR or ACM-A2 and the ones using ACM-PE is visible but less important.

The results from the tests using ACM-FR or ACM-A2 show globally the same trend, with a low heat release during the whole duration of the test, but not exceeding 300 kW. Composition ACM-A2 + MW gives the best results as expected, but the compositions with ACM-A2 + K15 and ACM-FR + MW gave close results.

On total heat release, higher values for tests using PIR compared with tests using K15 (approximately 5% more) probably indicate that PIR contributes more than K15 to energy released. They both contribute significantly more than MW.

In conclusion, for heat release, the largest contributor to the peak was the type of cladding when ACM-PE was used, with a little influence from the nature of the insulant during the decay phase. For the ACM-A2 and ACM-FR compositions, the insulants behaved broadly in a similar manner, especially compared against the performance of compositions integrating ACM-PE claddings.

6.3 | Temperatures and heat flux

All results of temperature measurements are available in Figure 8A to I. Considering a presence of the flame arbitrary at the surface or in the

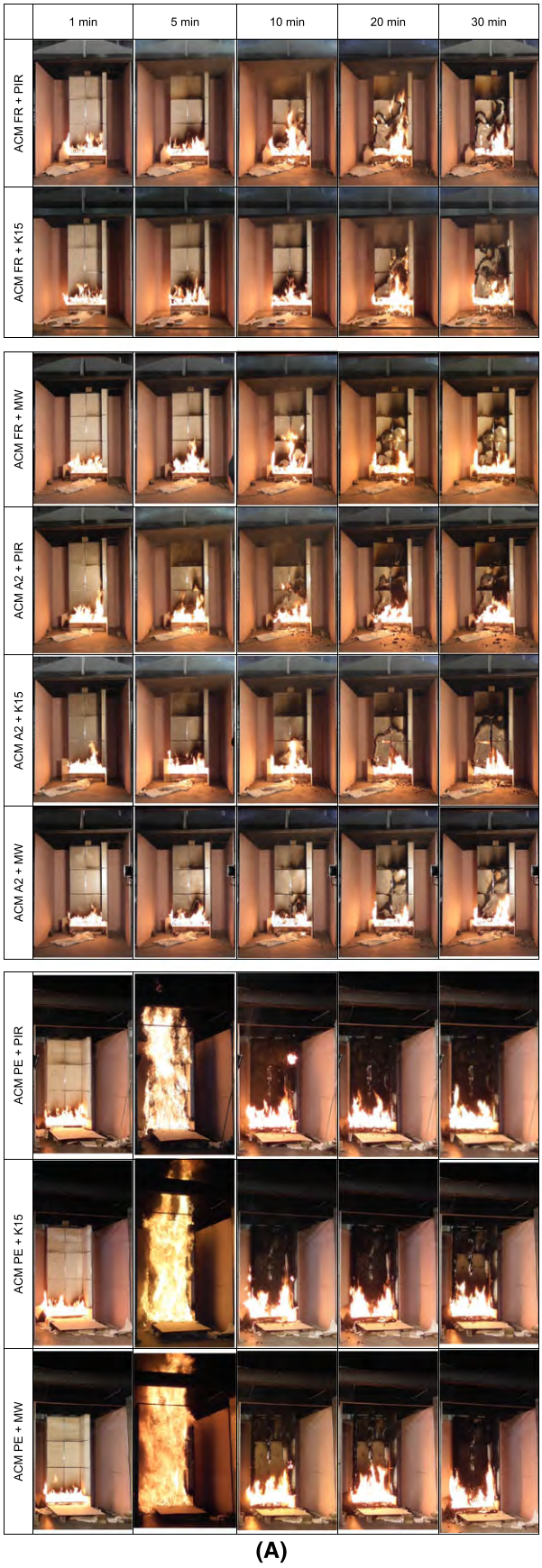

FIGURE 3 A, Observations during tests. B, Observations of insulants after tests [Colour figure can be viewed at wileyonlinelibrary.com]

FIGURE 3 Continued.

cavity corresponding to a temperature exceeding 400°C, several observations could be performed:

- For the test on the ACM-FR + PIR: the flame flashed on the cavity then reached 500 mm at around 7 minutes. Then, the flame progressed up the cladding, stopping at 1500 mm.
- For the test on ACM-FR + K15: after a very short flash, the flame was visible in the cavity after 10 minutes (LC1 position). On the cladding, the flame passed 500 mm only after 13 minutes and 1000 mm after 18 minutes.
- For the test on ACM FR + MW, there was less flash in the cavity. The flame front reached the 500-mm position before 7 minutes, then propagated to a maximum of 1500-mm position in the back wing and 1000 mm in the side wing.
- For the test on ACM A2 + PIR, flame is still quickly visible in the cavity. On the cladding, 500 mm was reached in less than 5 minutes, then the1000 mm position was reached in approximately 8 minutes.
- For the test on ACM A2 + K15: flame was quickly present in the cavity. The flame passed 500 mm after 4 minutes and progressed to reach 1500 mm at 15 minutes. All the other sensors remained under 300°C.
- For the test on ACM A2 + MW, flame presented quickly in the cavity. The flame passed 500 mm after 7 minutes and progressed to reach 1500 mm at 11 minutes.
- For the 3 compositions with ACM-PE, all sensors quickly grew over the limit; in less than 5 minutes, all the surfaces were ignited.

In all scenarios using ACM-A2 and ACM-FR, the cavity barrier was efficient, and the surface temperature was limited to a maximum of 1500 mm. When ACM-PE was used, all sensors showed generalised fire on the surface and in the cavity in a few minutes. In scenarios with ACM-FR, a criteria of 400°C was also reached on the side wall. This was not reached with ACM-A2.

Heat flux was measured on top of the sample as required in ISO 13785-1. No significant heat flux was measured from tests on compositions using ACM-FR and ACM-A2 claddings, and Figure 9 just highlights the results from tests with ACM-PE claddings. Results were similar to those observed for heat release: similar results for tests using ACM-PE claddings over PIR or K15 and a peak between 80 and 100 kW/m^2, and a less intense heat flux on ACM-PE + MW with a peak at 60 kW/m^2 and a shorter decay. The shape of the curve is similar to observations from heat release with a rapid growth after 4 minutes and a peak duration of only a few minutes. This corresponds mainly to the presence of a flame facing directly the heat fluxmeter.

6.4 | Smoke

For smoke measurement, it is difficult to remove the contribution from the burner, yet this contribution was considered as negligible. Results

TABLE 4 Heat release results

Cladding	ACM-FR			ACM-A2			ACM-PE		
Insulant	PIR	K15	MW	PIR	K15	MW	PIR	K15	MW
HRR max (kW)	397	280	298	306	244	194	5100	5159	4883
(without burner)	297	180	198	206	144	94	5000	5059	4783
THR (MJ)	438	412	360	421	387	318	848	821	636
(without burner)	258	232	180	241	207	138	668	641	456

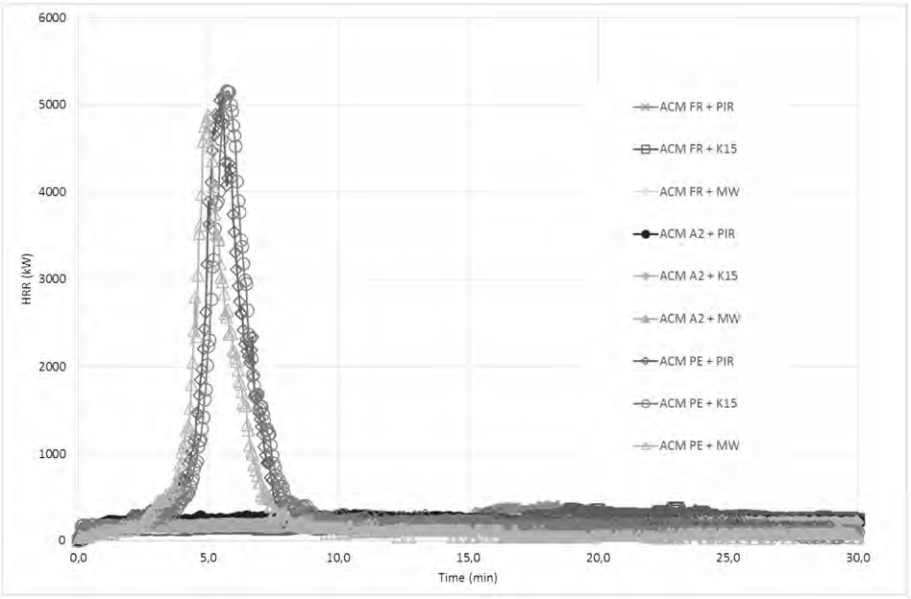

FIGURE 4 Heat release rate

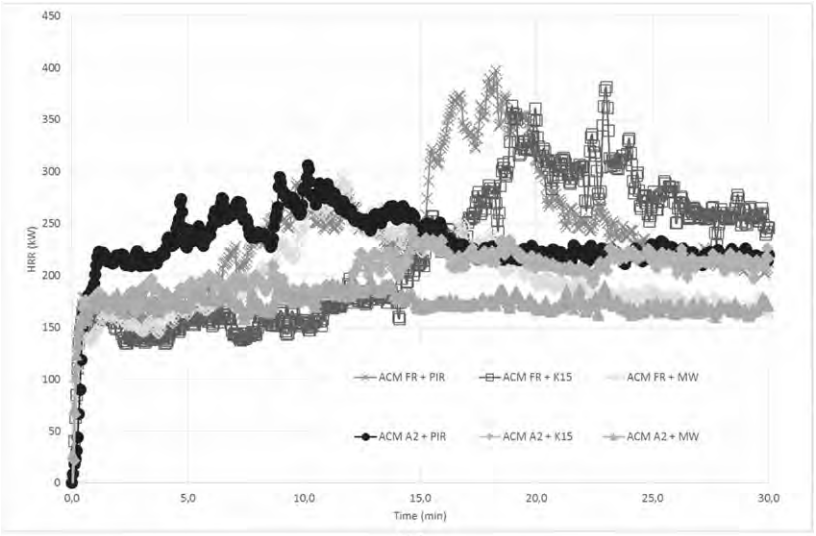

(A)

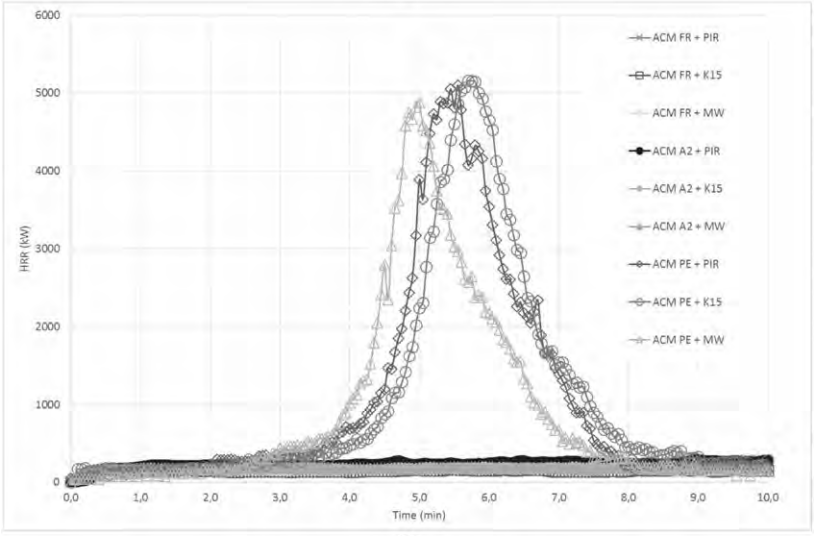

(B)

FIGURE 5 A, Heat release rate—zoom for tests on ACM-FR and ACM-A2. B, Heat release rate—zoom on first 10 minutes

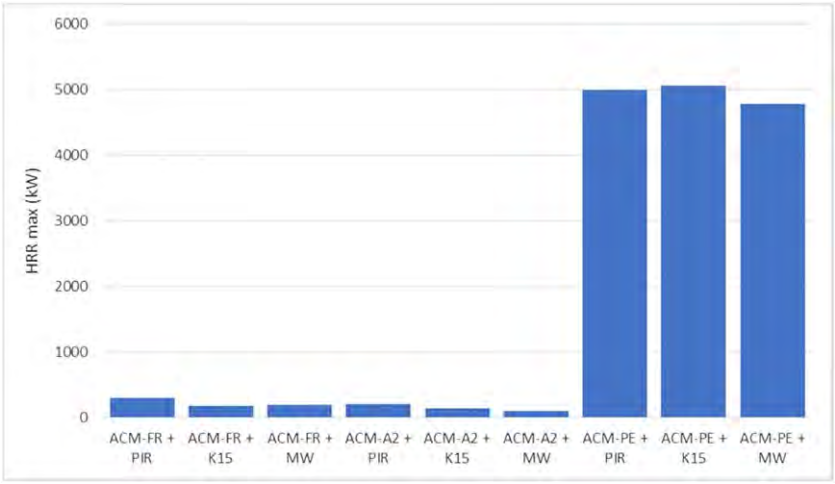

FIGURE 6 Maximum heat release rate (contribution of burner removed) [Colour figure can be viewed at wileyonlinelibrary.com]

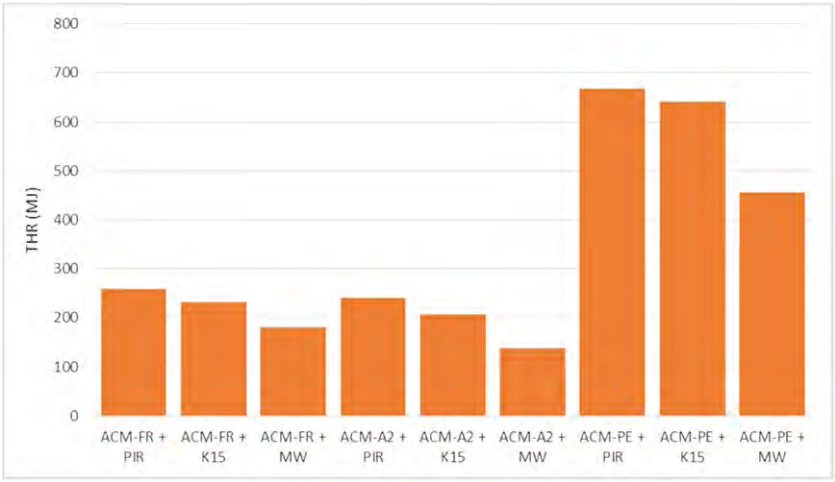

FIGURE 7 Total heat released (contribution of burner removed) [Colour figure can be viewed at wileyonlinelibrary.com]

are detailed in Table 5 and Figures 10 to 12 for rate of smoke production (RSP) and for total smoke production (TSP).

Results on RSP reveal again the peak observed for tests with ACM-PE claddings, but the difference is less visible than for the heat release rate. It means that the combustion phase corresponding to this phase, from 4 minutes to 8 minutes when ACM-PE is used, produces less smoke in proportion than the rest of the test. This is probably linked to a very intense combustion that re-burns all the smoke. PE combustion produces less smoke in proportion. This is also visible in the results for the total amount of smoke produced, where the difference between the tests was of less importance. In these results, tests that produce the smallest quantity of smoke were on ACM-FR + K15, ACM-FR + MW, and ACM-A2 + MW compositions. Tests using PIR seem to release more smoke than those with K15 and MW, but the difference was small.

6.5 | Gases evolved

Gases evolved was quantified using non-dispersive infrared analyser for carbon dioxide (CO_2) and electrochemical cell for CO. Other species have been measured using FTIR analyser and semi-quantitative analysis is presented.

6.5.1 | Carbon dioxide

The emission rate of carbon dioxide was calculated from the gas concentration in the duct and flow rate. This is presented in Table 6 and Figures 13 to 15. The contribution of the burner for carbon dioxide was removed in the table thereafter, considering stoichiometric combustion of propane and a flame of 100 kW, as per ISO 19703[32] formulas.

As for the other parameters, peak from tests using ACM-PE is very visible in maximum emission rate, but the proportion of carbon dioxide evolved over the heat release rate is less important than from the 6 other ones. It means that the fuel burning during the peak is more hydrogenated than all that is burning during the other tests. The products of pyrolysis of ACM-PE are light saturated hydrocarbons, compared with heavier fuels in the rest of the tests. For the total quantity of carbon dioxide evolved, the comparison shows less differences between tests, as all are averaged over 30 minutes. Note that uncertainty of measurement of small quantities of carbon dioxide after peak in tests using ACM-PE claddings is high, as measured values are close to the resolution of the larger calorimeter, leading to a risk of misinterpretation.

6.5.2 | Carbon monoxide

The emission rate of CO was calculated from gas concentration in the duct and flow rate. This is presented in Table 7 and

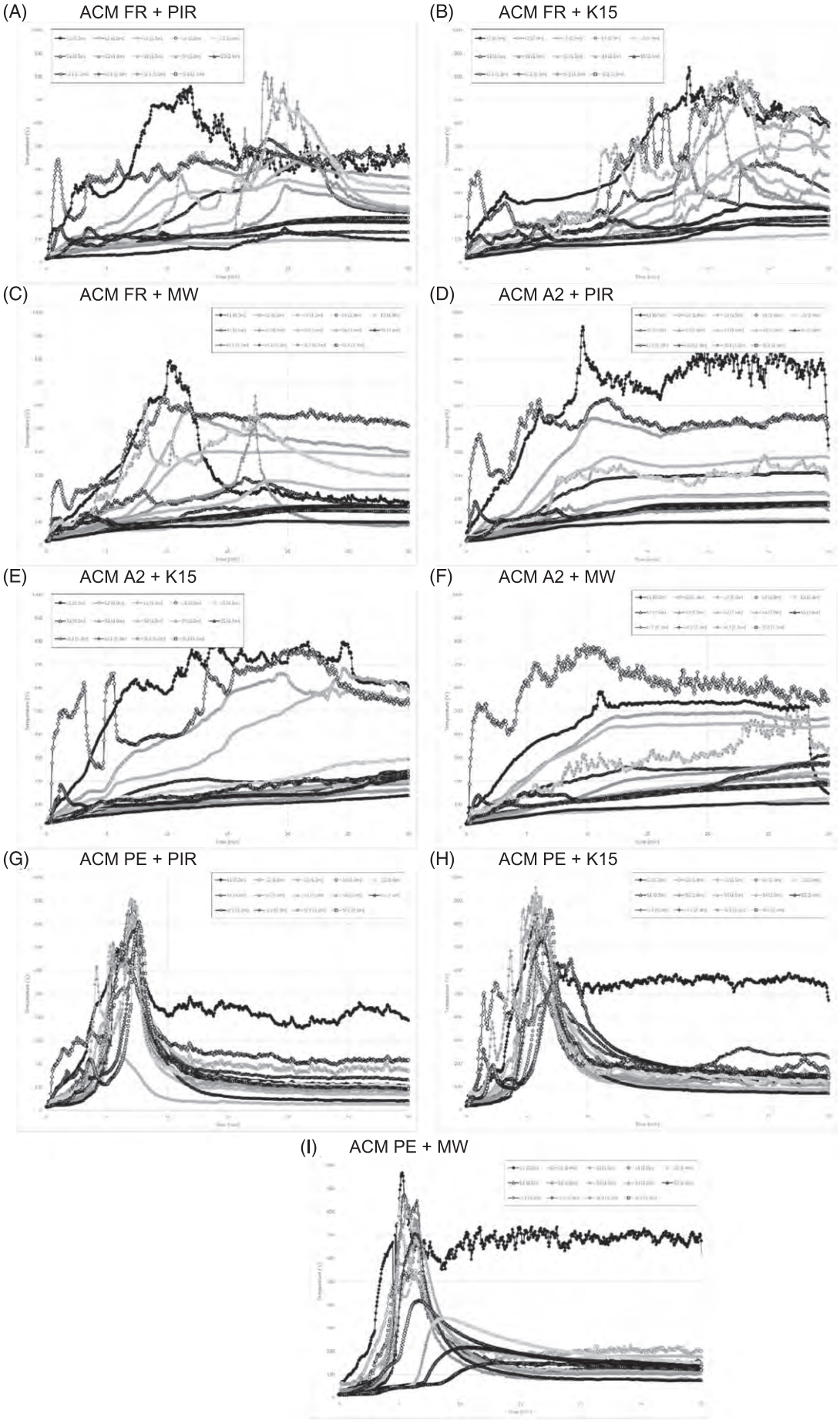

FIGURE 8 Temperature measurements

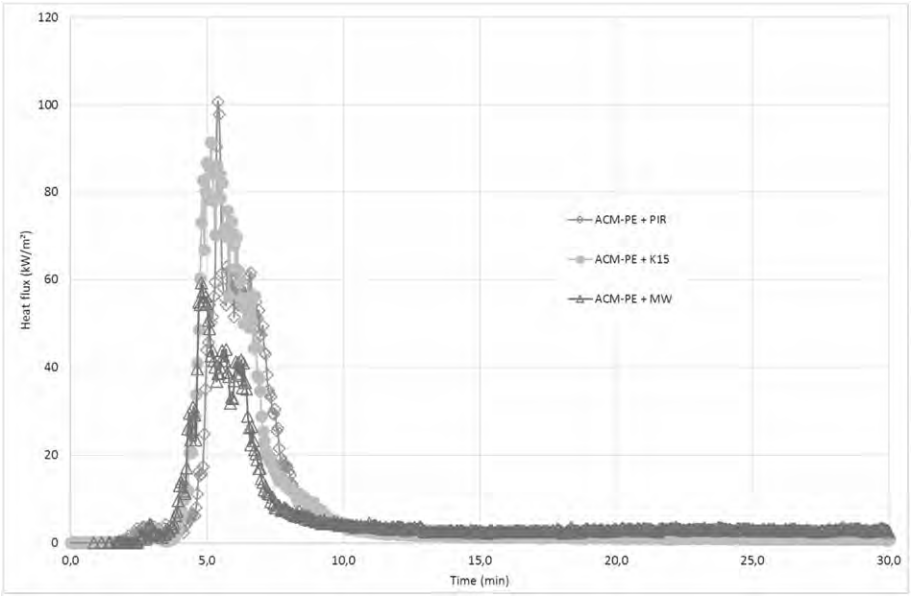

FIGURE 9 Heat flux—tests on ACM-PE compositions

TABLE 5 Smoke production results

Cladding	ACM-FR			ACM-A2			ACM-PE		
Insulant	PIR	K15	MW	PIR	K15	MW	PIR	K15	MW
RSP max (m^2/s)	4.6	1.8	2.6	7.4	3.3	0.9	21.8	23.0	18.5
TSP (m^2)	2290	1114	1270	2923	1850	1225	3110	3604	2614

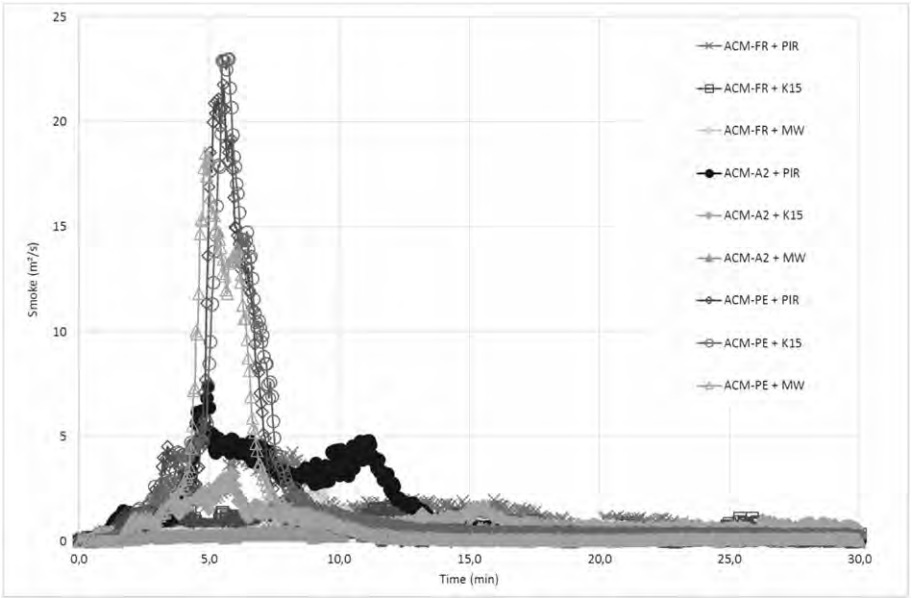

FIGURE 10 Rate of smoke production

Figure 16 to Figure 18. Figure presents semi-quantitative FTIR analysis, which is more resolved than measurement from the two other techniques.

Quantities of CO evolved are very small, leading to a limit in resolution for tests with ACM-PE claddings (visible as "steps" in Figure 16). The test on ACM-PE + MW is difficult to interpret as values are close to the limit of detection. This is due to the use of the large calorimeter and the very small quantity of CO evolved. Results are in the proper range of measurement for tests using ACM-FR and ACM-A2 claddings using small calorimetric hood. The ratio between CO and CO_2 plotted as Figure 19 shows a well-ventilated condition compared with the limit of 0.05 proposed as ISO 19706 criteria.[33]

Figure 20 presents results from semi-quantitative analysis using FTIR in range 2177.9 to 2174.5 cm^{-1} and corrected from interferences.

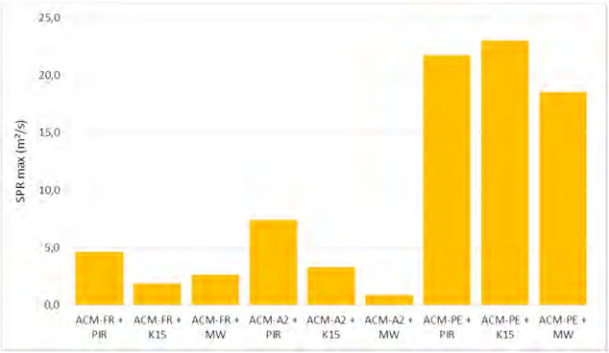

FIGURE 11 Maximum rate of smoke production [Colour figure can be viewed at wileyonlinelibrary.com]

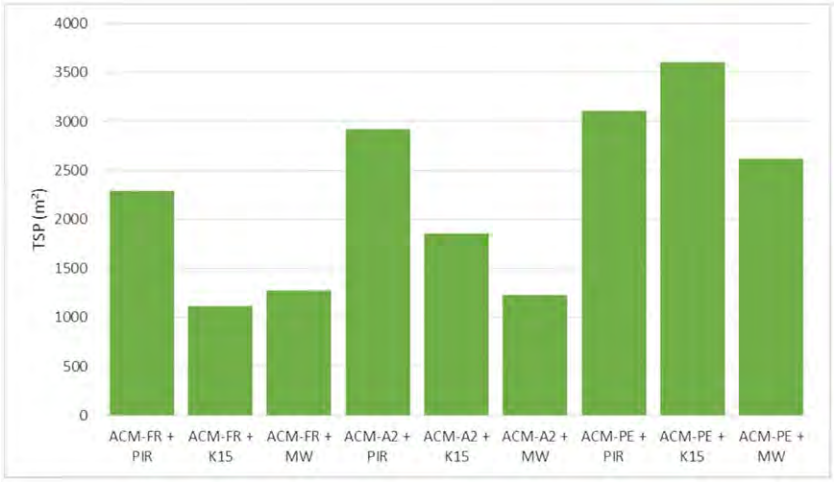

FIGURE 12 Total smoke produced [Colour figure can be viewed at wileyonlinelibrary.com]

TABLE 6 Carbon dioxide production results

Cladding	ACM-FR			ACM-A2			ACM-PE		
Insulant	PIR	K15	MW	PIR	K15	MW	PIR	K15	MW
CO_2 max (g/s)	70.2	67.3	38.8	39.0	31.0	22.8	260.3	259.9	275.2
CO_2 total (kg)	65.6	53.6	42.7	50.2	48.6	36.8	64.5	71.8	60.3
(without burner)	53.9	41.9	31.1	38.5	37.0	25.2	52.9	60.2	48.7

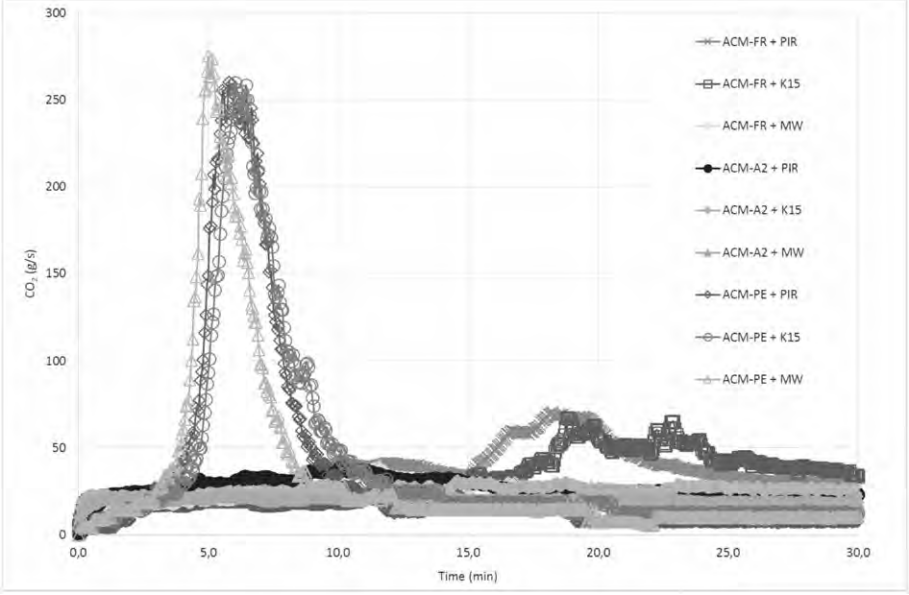

FIGURE 13 Carbon dioxide evolved

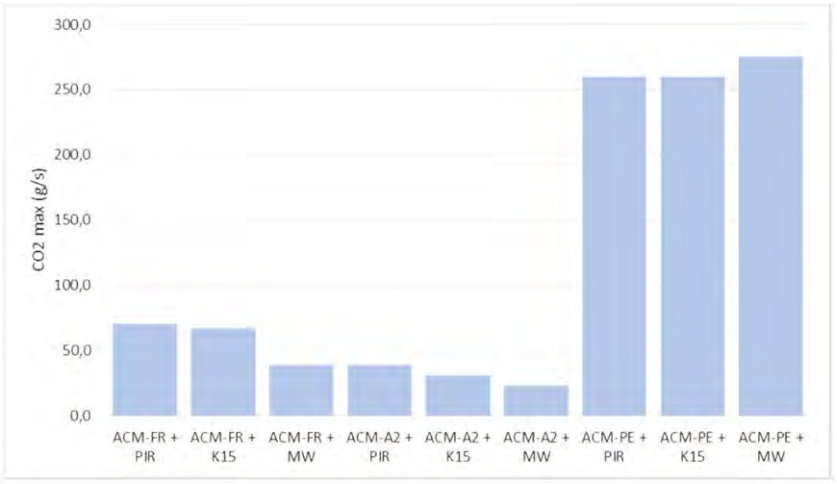

FIGURE 14 Carbon dioxide maximum emission rate (contribution of burner removed) [Colour figure can be viewed at wileyonlinelibrary.com]

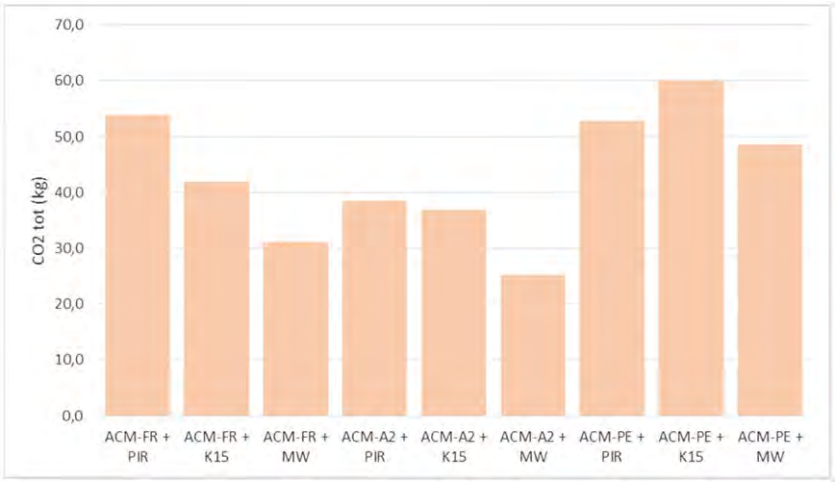

FIGURE 15 Carbon dioxide total mass released (contribution of burner removed) [Colour figure can be viewed at wileyonlinelibrary.com]

TABLE 7 Carbon monoxide production results

Cladding	ACM-FR			ACM-A2			ACM-PE		
Insulant	PIR	K15	MW	PIR	K15	MW	PIR	K15	MW
CO max (g/s)	0.808	0.956	0.832	1.008	0.871	0.340	2.952	3.089	0.648
CO total (kg)	0.859	1.006	0.538	0.891	1.036	0.341	0.317	0.386	0.079

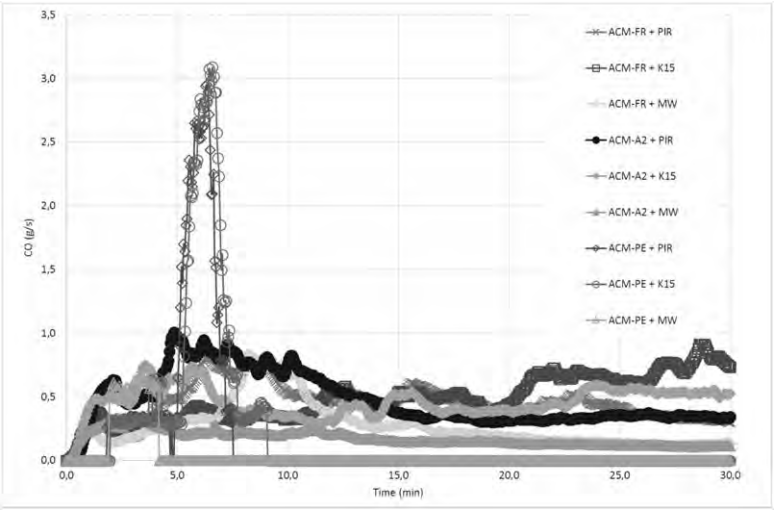

FIGURE 16 Carbon monoxide production rate

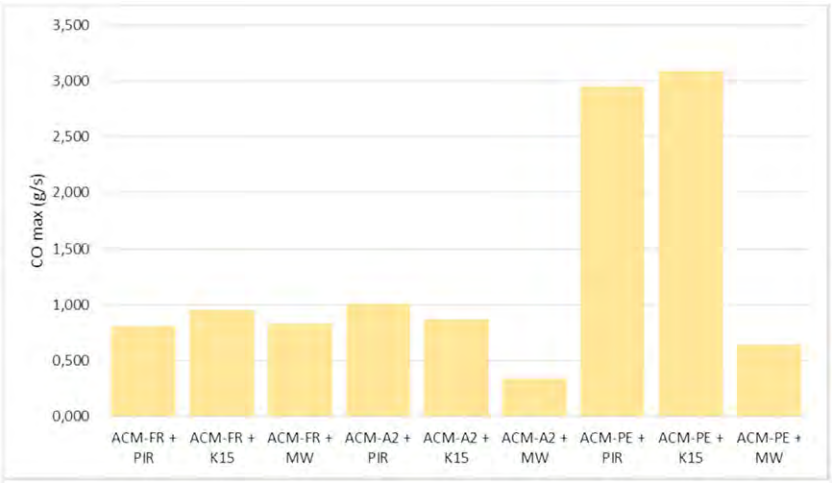

FIGURE 17 Carbon monoxide maximum emission rate [Colour figure can be viewed at wileyonlinelibrary.com]

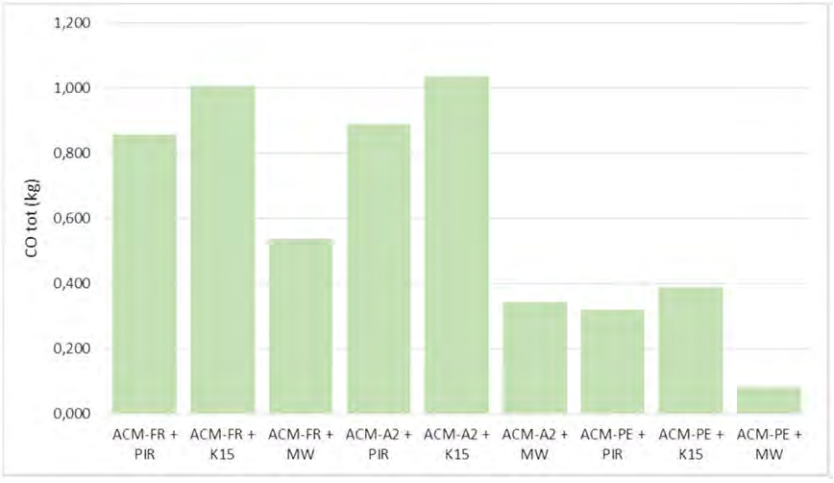

FIGURE 18 Carbon monoxide total mass released [Colour figure can be viewed at wileyonlinelibrary.com]

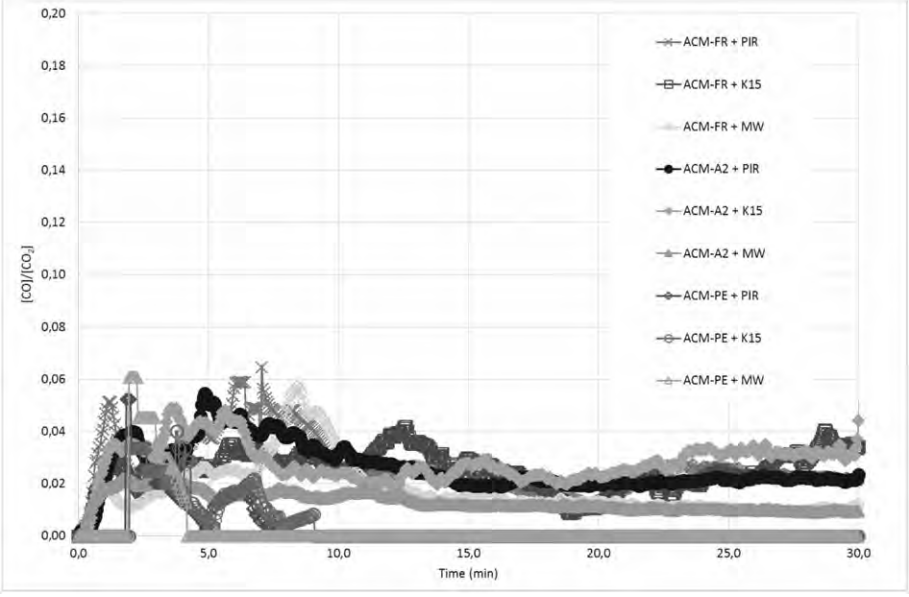

FIGURE 19 $[CO]/[CO_2]$ ratio

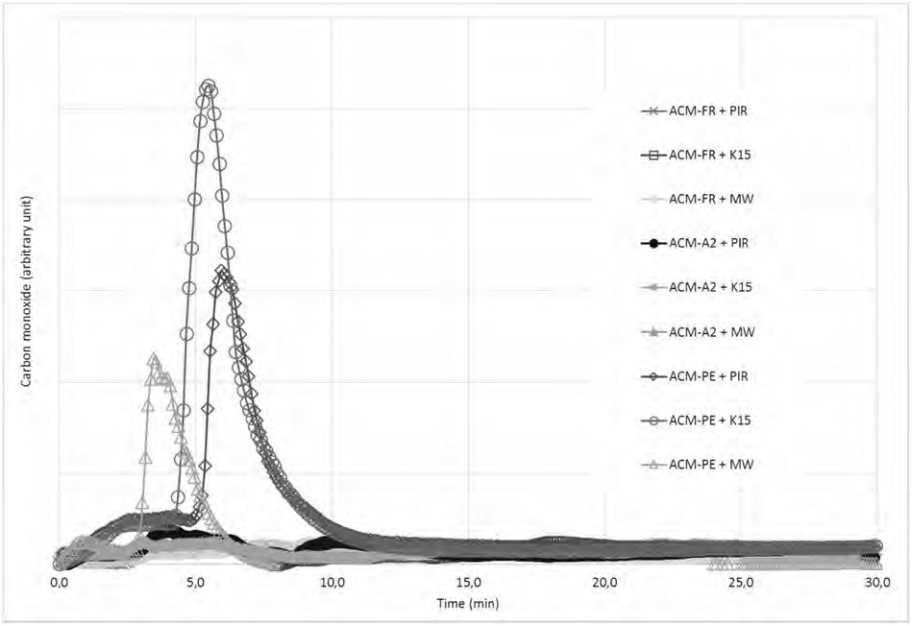

FIGURE 20 Carbon monoxide semi-quantitative analysis using FTIR

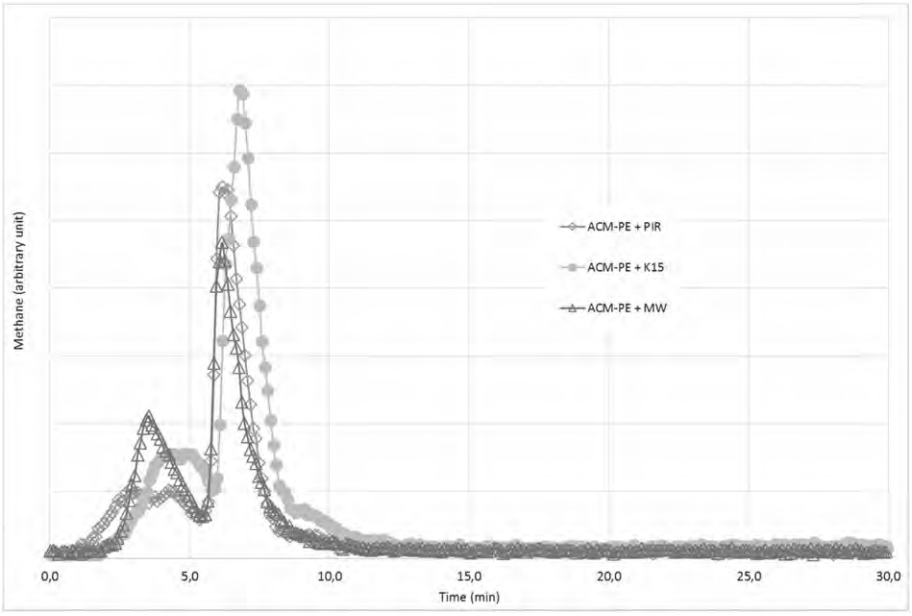

FIGURE 21 Methane released, tests on ACM-PE compositions (band at 2951.1-2946.7 cm^{-1})

Trends show CO produced mainly in the decay phase for tests ACM-PE + K15 and ACM-PE + PIR and improve the resolution of the peaks compared with Figure 16. CO produced in test on ACM-PE + MW is lower, and this probably explains the difficulty to resolve it with the electrochemical cell in Figure 16. As a conclusion for CO, quantities evolved are very small, including during the peak of the 3 tests on ACM-PE, meaning a well-ventilated and very rich combustion.

6.5.3 | Other species

FTIR analysis performed during the tests has proven the presence of unburnt hydrocarbons in the smoke. Evidence of methane, ethylene, acetylene, and propane was highlighted during intense combustion in tests using ACM-PE claddings and visible for methane and ethylene, respectively, in Figures 21 and 22. The double peak visible for these tests frames the most intense period of combustion visible in heat release curve of Figure 5. This means that there is a first period of smoke rich in pyrolysis gases, followed by the most intense period of combustion, where concentrations of methane and ethylene fall down, meaning that the fire is so intense that the large majority of pyrolysis gases in the effluents are burnt. During the last period, the heat release intensity is decreasing, leading to a second peak of unburnt fuel in the effluents. Methane is also visible as traces in all other tests.

No traces of hydrogen cyanide was found in any test, or any other nitrogen-containing species. This means that contribution of insulants,

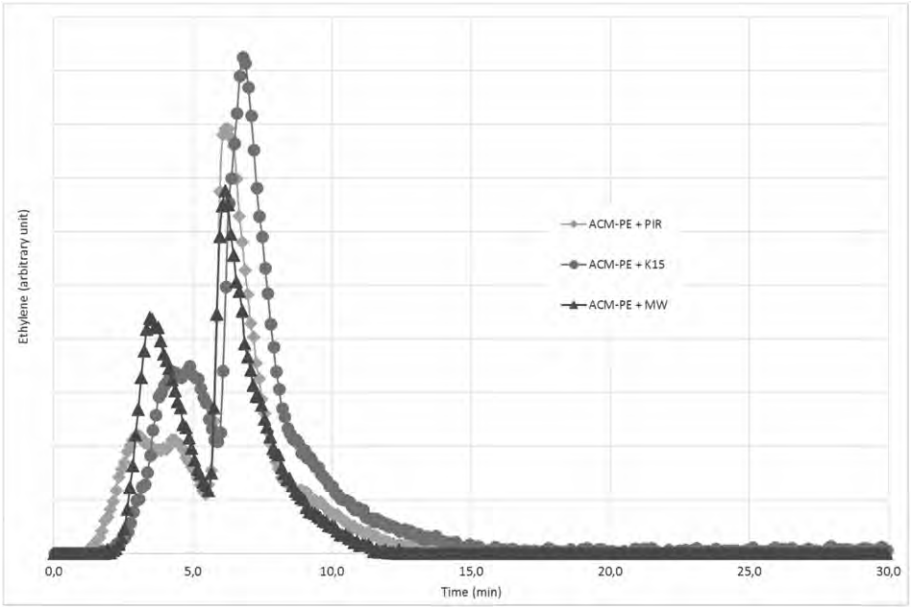

FIGURE 22 Ethylene released, tests on ACM-PE compositions (band at 2988 cm^{-1})

and especially PIR, is not visible in terms of species production, even in the largest fires involving ACM-PE claddings. Qualitative analysis performed in addition highlighted the possible presence in insignificant quantities of formaldehyde in test on ACM-PE + MW.

7 | CONCLUSIONS

Tests performed are discriminant between solutions. They highlight that, for tested compositions, the cladding is the most important parameter driving global fire behaviour. ACM-PE-based cladding systems gave very different results from the other solutions tested. This was especially visible in heat release rates, where fire intensity was very high, whatever the insulant used in the system. The contribution of the insulant was only remarkable in these tests during the decay phase. The cavity barrier was largely ineffectual in the 3 tests with ACM-PE cladding, as the integrity of the cavity was not ensured.

Additional gas analyses highlighted a very well-ventilated condition of combustion with the ACM-PE-based cladding compositions, probably enforced by the test setup and entrainment inside the cavity. Carbon monoxide release was low in proportion. Hydrocarbon release was remarkable, but no other species was detected within the limits of detection achievable in this setup.

For the solutions with ACM-FR and ACM-A2 claddings, the results for all of the insulants trended in a similar manner in these test conditions, especially when compared with the performance of ACM-PE-based compositions.

In these tests and tested compositions, the cladding was the governing part of the constructive system, and the contribution of insulants remained low in terms of energy or gases evolved. This confirms BRE tests according to BS 8414-1 and supplements the results with gases evolved and heat released from the beginning to 30 minutes without external action such extinction. These tests highlight also, that the BRE tests might have developed much more higher with the ACM-PE cladding, if they had not been extinguished. For such constructive systems, use of intermediate-scale tests is a very powerful tool to complete any reference real-scale test, for example in the case of extended applications.

Unfortunately, intermediate scale tests as well as the reference BS8414-1 test do not cover all the details of a façade constructive system and single points, such as window frames, could have an important effect. Their effects on fire behaviour of the facade require further evaluation.

ACKNOWLEDGEMENT

The authors would like to thank Kingspan BV to allow us to use the results of their testing for this paper. Authors thank also Maurice McKee and William Veighey for their work performing these tests.

ORCID

Eric Guillaume http://orcid.org/0000-0002-3055-2741
Talal Fateh http://orcid.org/0000-0002-4204-0540

REFERENCES

1. Facades market analysis by product (ventilated, non-ventilated), by end use (commercial, residential, industrial), by region (North America, Europe, Asia Pacific), and segment forecasts, 2014–2025. Report ID: GVR-1-68038-221-1. Published Nov, 2017.
2. Cladding market analysis by product (steel, aluminum, composite panels, fiber cement, terracotta, ceramic), by application, competitive landscape, and segment forecasts, 2014–2025. Report ID: GVR-1-68038-477-2. Published Jun, 2017.
3. Valiulis J. Building exterior wall assembly flammability: have we forgotten the past 40 years? In fire Engineering Magazine, November 2015.
4. White N, Delichatsios M. Fire hazards of exterior wall assemblies containing combustible components. FPRF final report, project FE2568, Quincy, MA, USA. 2004.
5. White N, Delichatsios M, Ahrens M, A. Kimball. Fire hazard of exterior wall assemblies containing combustible components. Proceedings of 1st international seminar for fire safety of facades., Paris. 2013:77–88.

6. Interim report into the Review of Building Regulations and Fire Safety. UK Department for Communities and Local Government, issued 18 December 2017 https://www.gov.uk/government/news/interim-report-into-the-review-of-building-regulations-and-fire-safety
7. BS 8414–1:2015+A1:2017. Fire performance of external cladding systems. Test method for non-loadbearing external cladding systems applied to the masonry face of a building
8. BR135. Colwell S, Baker T. Fire performance of external thermal insulation for walls of multistorey buildings, 3rd edition, IHS/BRE
9. Collection: Grenfell Tower UK Department for Communities and Local Government, Last Update 22 November 2017 https://www.gov.uk/government/collections/grenfell-tower
10. BRE. Fire test report: DCLG BS 8414 Test. 2017;1:7 August.
11. BRE. Fire test report: DCLG BS 8414 Test. 2017;2:3 August.
12. BRE. Fire test report: DCLG BS 8414 Test. 2017;3:8 August.
13. BRE. Fire test report: DCLG BS 8414 Test. 2017;4:11 August.
14. BRE. Fire test report: DCLG BS 8414 Test. 2017;5:14 August.
15. BRE. Fire test report: DCLG BS 8414 Test. 2017;6:25 August.
16. BRE. Fire test report: DCLG BS 8414 Test. 2017;7:21 August.
17. Agarwal G. Research Technical Report: evaluation of the fire performance of aluminum composite material (ACM) assemblies using ANSI/FM 4880. FM Global, Norwood, MA02062, USA, December 2017.
18. NFPA 285. Standard fire test method for evaluation of fire propagation characteristics of exterior non-load-bearing wall assemblies containing combustible components. 2012.
19. ISO 13785–1:2002. Reaction-to-fire tests for façades—Part 1: Intermediate-scale test.
20. ISO 24473:2008. Fire tests—open calorimetry—measurement of the rate of production of heat and combustion products for fires of up to 40 MW.
21. ISO 16405:2015. Room corner and open calorimeter—guidance on sampling and measurement of effluent gas production using FTIR technique.
22. ISO 19702:2015. Guidance for sampling and analysis of toxic gases and vapours in fire effluents using Fourier Transform Infrared (FTIR) spectroscopy
23. ISO 9705-1:2016. Reaction to fire tests—room corner test for wall and ceiling lining products—Part 1: Test method for a small room configuration.
24. EN 13238:2012. Reaction to fire tests for building products—conditioning procedures and general rules for selection of substrates.
25. ISO 14934-1:2010. Fire tests—calibration and use of heat flux meters—part 1: general principles.
26. Thornton W. The relation of oxygen to the heat of combustion of organic compounds. *Philosophical Magazine and J of Science*. 1917;33(194):196-203.
27. Huggett C. Estimation of rate of heat release by means of oxygen consumption measurements. *Fire Mater*. 1980;12(2):61-65.
28. Janssens ML. Measuring rate of heat release by oxygen consumption. *Fire Technol*. 1991;27(3):234-249.
29. ISO 19701:2013. Methods for sampling and analysis of fire effluents.
30. ISO 19702:2015. Guidance for sampling and analysis of toxic gases and vapours in fire effluents using Fourier Transform Infrared (FTIR) spectroscopy.
31. Guillaume E, Saragoza L. Application of FTIR analyzers to fire gases—progress in apparatus and method validation for quantitative analysis. Fire and materials 2015, San Francisco, USA, 2–4 Feb 2015.
32. ISO 19703:2010. Generation and analysis of toxic gases in fire—calculation of species yields, equivalence ratios and combustion efficiency in experimental fires.
33. ISO 19706:2011. Guidelines for assessing the fire threat to people.

How to cite this article: Guillaume E, Fateh T, Schillinger R, Chiva R, Ukleja S. Study of fire behaviour of facade mock-ups equipped with aluminium composite material-based claddings, using intermediate-scale test method. *Fire and Materials*. 2018;1–17. https://doi.org/10.1002/fam.2635